Arab J Sci Eng (2017) 42:4391–4400
DOI 10.1007/s13369-017-2472-8

RESEARCH ARTICLE - CHEMISTRY

Effect of Co-ions on Cr(VI) and F^- Adsorption by Thermally Treated Bauxite (TTB)

M. R. Ghosh[1] · **S. P. Mishra**[1]

Received: 12 November 2016 / Accepted: 6 March 2017 / Published online: 25 March 2017

Abstract A low-cost material bauxite is activated thermally and that thermally treated bauxite (TTB) has been used to adsorb Cr(VI) and F^- ions separately from aqueous solution in batch methods. The optimum condition for adsorption is stirring speed—200 rpm for both, contact time—120 min for Cr(VI) and 180 min for F^-, temperature—30 °C for both, pH—2 to 3 for Cr(VI) and 2 to 8 (very little variation) for F^-. All the kinetic models used for adsorption studies such as Freundlich, Langmuir, Lagergren, Ho and Mc-kay, Dubinin–Radushkevich (D.R.), Webber Morris, Temkin isotherms have been tested with the experimental data. The nature of both the adsorption processes is similar in all respects. The main finding in this paper is the effect of presence of both cationic (Na^+, Mg^{2+} and Al^{3+}) and anionic (Cl^-, SO_4^{2-}, PO_4^{3-}) co-ions on Cr(VI) or F^- adsorption. Cr(VI) or F^- adsorption on TTB is affected by the presence of both cationic and anionic co-ions. In both Cr(VI) and F^- adsorptions, it has been observed that interference increases with the increase in size of both the types of ions and charge on the anions. Similarly, it decreases with the increase in charge on the cations.

Keywords Thermodynamic parameters · Pzc · Adsorption isotherms · Co-ions · Ionic strength · FTIR

1 Introduction

Nowadays, environmental pollution is one of the most important issues facing humanity. In the past few years, it was increased epidemically and reached panic levels in terms of its effects on living beings. Toxic heavy metals are regarded as one of the pollutants that have direct effect on human beings and animals [1]. The industrial activities such as tanning, metallurgical operation, mining, electroplating and manufacturing are the causes of release of heavy metals and other toxic elements into the environment [2]. Unlike the organic pollutants which are biodegradable, toxic elements like Cr(VI), F^- and other heavy metal ions are not biodegradable [3], therefore, making them a source of great concern.

Usually, chromium exists in the aqueous solution in two stable forms Cr(III) and Cr(VI). Among them, Cr(III) acts as an important trace element in plants and animal metabolism. On the contrary, Cr(VI) is found to be toxic, mutagenic and carcinogenic [4]. The most electronegative element fluorine is distributed ubiquitously as fluorides in nature [5]. At low concentration ($\cong$1 mg/L), F^- prevents dental caries, whereas at high concentration it causes skeletal fluorosis. The Indian standard of F^- in drinking water is 1.5 mg/L. Water is the main source of fluoride intake by humans [6]. Therefore, in country like India, the problems associated with excess fluoride in drinking water are highly endemic [7]. The pollution due to the combined effect of hexavalent chromium and fluoride in water bodies causes mass environmental concern, and therefore its treatment is of utmost importance. These toxic elements enter our body through drinking, eating, inhaling, eye and skin contact. The damage that they do is on the cellular level and can cause cancer and many other diseases [8]. Due to the toxicological effects of these elements, interest in heavy metals and other toxic elements removal from wastewater has been on the rise.

Several methods have been developed to remove heavy metals and other toxic elements from wastewater before release into the water bodies. These methods are precipitation, reduction, ion exchange, reverse osmosis, dialysis and adsorption. Most of these methods are expensive so are not

✉ S. P. Mishra
spm_iter@rediffmail.com

[1] Department of Chemistry, Siksha 'O' Anusandhan University, Bhubaneswar 751 030, India

affordable for a developing country like India. They also have very limited applications because they cannot remove metals at low concentration [9].

So, adsorption method is being given priority nowadays [10–12]. Use of natural adsorbents in the adsorption processes is being given more importance because of their easy availability and low cost. Adsorption of heavy metals and other toxic elements onto adsorbents can be affected by the surrounding environmental conditions, such as pH, background electrolyte composition or ionic strength [13]. Several types of background electrolyte ions are present over a wide range of concentrations in natural or wastewater systems. The concentration and type of electrolyte ions depend on the source of water [14]. These electrolytes provide cations and anions which interfere in the adsorption processes. Generally, co-cations interfere with the positively charged adsorbates and co-anions interfere with the negatively charged adsorbates. Co-anions may also form water-soluble metal-anion complexes or precipitates if heavy metal ions are present in the aqueous system [15]. Therefore, in the present study effect of co-ions (both cations and anions) on Cr(VI) or F^- adsorption onto a low-cost natural mineral bauxite has been tested by adding different electrolytes such as $NaNO_3$, $Mg(NO_3)_2 \cdot 6H_2O$, $Al(NO_3)_3 \cdot 9H_2O$, NaCl, Na_2SO_4 and Na_2HPO_4 $.2H_2O$ to the solution containing either Cr(VI) or F^- ions. These are the electrolytes which ionize to different cations and anions in aqueous solution. Bauxite was chosen basing on a preliminary study using various other natural low-cost adsorbents and minerals.

2 Experimental

2.1 Preparation of Adsorbent and Adsorbate

Bauxite used in this study was procured from Hydro and Electrometallurgy division of Institute of Minerals and Materials Technology, Bhubaneswar (A CSIR laboratory). The same was collected from Panchpatmali of Koraput district in Odisha. The material was powdered and dried at 110 °C overnight. The 150 μm size fraction of the material was taken for adsorption studies. The required amount of bauxite for heat activation was placed in a crucible and heated in a muffle furnace at four different temperatures (200, 400, 600, 700 °C) for 2 h. These temperatures were selected haphazardly. Then, the sample was cooled and kept in a desiccator containing silica gel for further use. Stock solution of 1000 mg/L of Cr(VI) or F^- was prepared using requisite quantity of $K_2Cr_2O_7$ or NaF of analytical grade in acidified distilled water. During batch adsorption experiments, the stock solution was diluted to the required concentration level needed for the adsorption studies.

2.2 Characterization of the Sample

Fourier transform infrared (FTIR) spectra of the adsorbent before/after modification and after adsorption were determined using JASCO FTIR instrument-4100. The samples were pressed into spectroscopic quality KBr pellet with a sample/KBr ratio of about 1/100. The FTIR spectra were observed in the range of 4000–400 cm^{-1} frequency. By using KBr method [16], the pH at point of zero charge (pzc) of the adsorbent was determined. All other physicochemical parameters were determined by following the methods reported earlier [17].

2.3 Batch Adsorption Study

Batch experiments were done in 250-mL stoppered conical flasks containing 100 mL of solution containing either Cr(VI) or F^- ion. The pH of the solution was maintained by adding either 0.1 N HCl or 0.1 N NaOH solution. Stirring was carried out by a temperature-controlled magnetic stirrer. Samples were taken at regular time intervals and filtered through Whatman filter paper (no.1), and filtrate was analyzed for remaining Cr(VI) or F^- concentrations. Maximum adsorption experiments were conducted in the following conditions: contact time - 120 min for Cr(VI) and 180 min for F^-, pH—5.0, stirring speed—200 rpm, initial Cr(VI)/F^- concentration—10 mg/L, temperature—30 °C, adsorbent concentration—5 g/L. The temperature experiments were carried out by using a temperature-controlled thermostat. Each experiment was carried out in triplicate in order to get the repeated results. The mean value was taken for calculation.

The uptake was calculated according to Eq. (1) as follows:

$$q = (C_o - C_e)V/M \tag{1}$$

where q amount of Cr(VI)/F^- ions adsorbed per unit weight of adsorbent (mg/g) at equilibrium, C_o initial concentration of Cr(VI)/F^- (mg/L), C_e equilibrium concentration of Cr (VI)/F^- (mg/L), V volume of the solution in the reactor (L), M mass of the adsorbent (g)

$$\text{Sorption } (\%) = [(C_o - C_e)/C_o] \times 100 \tag{2}$$

2.4 Effect of Co-ions

For the study of co-ion effect, different electrolytes such as $NaNO_3$, $Mg(NO_3)_2 \cdot 6H_2O$, $Al(NO_3)_3 \cdot 9H_2O$, NaCl, Na_2SO_4 and Na_2HPO_4 $.2H_2O$ (0.01–0.15 M) were added separately to a solution containing either Cr(VI) or F^- ions (10 mg/L) and the adsorption studies were conducted at an adsorbent/adsorbate ratio of 10 g/L.

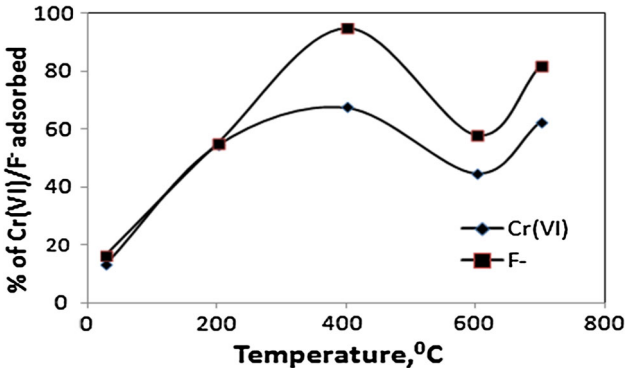

Fig. 1 % of $Cr(VI)/F^-$ adsorption by TTB treated at different temperatures

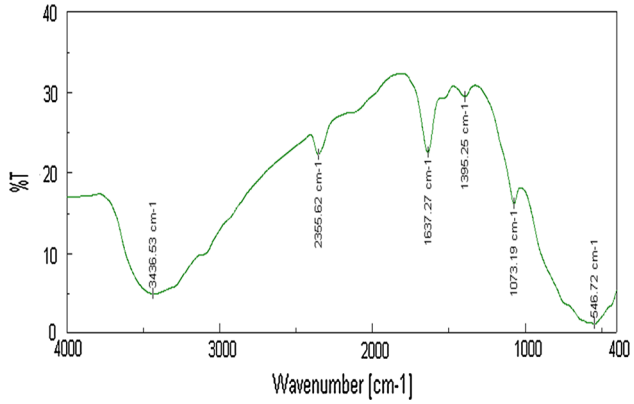

Fig. 2 FTIR spectra of TTB

2.5 Analysis

The concentrations of Cr(VI) or F^- in the solution before and after adsorption were determined by Elico SL-244 double beam UV–visible spectrophotometer following diphenyl carbazide (DPC) method [18] or sodium 2-parasulfophenylazo-1,8-dihydroxy-3,6-naphthalene sulfonate (SPADNS) method [19], respectively.

3 Results and Discussion

3.1 Modification of Raw Bauxite

Adsorption of Cr(VI) or F^- separately on untreated bauxite surface was found to be very less [13.2% for Cr(VI) and 16.5% for F^-]. So, in order to improve the adsorption percentage the bauxite surface was activated thermally [20]. Bauxite treated at 400 °C gave best result [68% for Cr(VI) and 95% for F^-] as shown in Fig. 1. That thermally (400 °C) treated bauxite (TTB) was used for further studies. Higher adsorption % at higher temperature modified bauxite may be due to the increase in porosity and surface area after removal of moisture and volatile substances present on bauxite surface after heat treatment. The % of both Cr(VI) and F^- adsorptions by TTB treated at temperatures higher than 400 °C again decreased, which may be due to the formation of more compact mineral phase such as corundum (Al_2O_3) [21].

3.2 Characterization of Bauxite

The surface of heat modified bauxite was analyzed by Fourier transform infrared (FTIR) spectroscopy, and the result is shown in Fig. 2. The strong and broad peak at 3436.5 cm^{-1} indicates hydroxyl (–OH) group. So, it is assumed that –OH is the major functional group present on the bauxite surface. Apart from this, other minor functional groups present are carbonyl groups (C–O) of alcohols and carboxylic acids, aluminum or silicon oxide corresponding to the wave no. 546.72 cm^{-1}. A medium peak has been observed at 2355.62 cm^{-1} may be due to sodium metasilicate Na_2SiO_3, $5H_2O$ [22]. FTIR graphs of both Cr(VI) and F^--loaded bauxite look same (graphs not shown), indicating the nature of both the adsorptions are almost similar. The negative peaks at 2355.62 cm^{-1} are converted to positive peaks in both the cases after adsorption.

$K_2Cr_2O_7$ is soluble in water and on dissolution it ionizes to K^+ and $Cr_2O_7^{2-}$ ions. $Cr_2O_7^{2-}$ reacts with water to give $HCrO_4^-$ or CrO_4^{2-} [23] as shown in Eqs. 3–5. So, $HCrO_4^-$ or CrO_4^{2-} are the two main forms of Cr(VI) in aqueous solution. Similarly, F^- exists as either fluoride (F^-) or bifluoride (HF_2^-) in aqueous solution. So, the formation of surface complexes in between TTB surface and negatively charged Cr(VI) or F^- ions may be assumed according to the following reactions.

$$K_2Cr_2O_7 \rightarrow 2K^+ + Cr_2O_7^{2-} \quad (3)$$

$$Cr_2O_7^{2-} + H_2O \leftrightarrow 2HCrO_4^- \quad (4)$$

$$Cr_2O_7^{2-} + H_2O \leftrightarrow 2CrO_4^{2-} + 2H^+ \quad (5)$$

$$S{-}OH + H^+ + HCrO_4^- \leftrightarrow S{-}OH_2^+{-}HCrO_4^- \quad (6)$$

$$2S{-}OH + 2H^+ + CrO_4^{2-} \leftrightarrow (S{-}OH_2^+)_2{-}CrO_4^{2-} \quad (7)$$

$$S{-}OH + H^+ + F^- \leftrightarrow S{-}OH_2^+{-}F^- \quad (8)$$

$$S{-}OH + H^+ + HF_2^- \leftrightarrow S{-}OH_2^+ - HF_2^- \quad (9)$$

where S–OH is the surface of adsorbent containing hydroxyl group and $S{-}OH_2^+{-}HCrO_4^-$, $(S{-}OH_2^+)_2{-}CrO_4^{2-}$, $S{-}OH_2^+{-}F^-$ and $S{-}OH_2^+{-}HF_2^-$ are the surface complexes [24]. Apart from these, hydroxyl groups present on TTB surface may get substituted by negatively charged ions of Cr(VI) or F^-. So, the formation of surface complexes and substitution reactions are the key factors of both Cr(VI) and F^- adsorption on TTB surface. Other physicochemical parameters were found to be point of zero charge (pzc)—7.8, pH—6, moisture content—3.3 %, loss of mass

on ignition—10.6 %, bulk density—1.66 g/mL and surface area—71 m^2/g.

3.3 Effect of Different Parameters

200 rpm stirring speed was found to be the optimum. Cr(VI) and F^- adsorptions on TTB surface were carried out by varying only the contact time keeping all other parameters constant (pH—5, stirring speed—200 rpm, initial Cr(VI) or F^- concentration—10 mg/L, temperature—30 °C, adsorbent concentration—5 g/L). As observed by other researchers [25], here also % of Cr(VI) and F^- adsorptions increase at the initial stage and after 120 and 180 min for Cr(VI) and F^-, respectively, adsorption percentage remain unchanged. So, 120 and 180 min contact periods were taken as optimum for Cr(VI) and F^- adsorptions, respectively.

In order to know the effect of pH on Cr(VI) and F^- adsorption by TTB, pH of the solution was varied from 2 to 10 keeping all other parameters constant. Adsorption was maximum at pH 2 to 3 for Cr(VI), and there was very little variation in adsorption from pH 2 to 8 in the case of F^-. At higher pH, % of adsorption decreased in both the cases as observed in Fig. 3. Because the bonds formed between carbonyl and hydroxyl groups present on TTB surface and Cr(VI) or F^- are comparatively weaker in basic solution [26]. In the acidic pH also, the formation of surface complexes as described earlier (Eqs. 6–9) is accelerated. So, % of adsorption is more in acidic pH. Another important reason for more adsorption in acidic pH is point of zero charge (pzc). The pzc of TTB is 7.8. So, below pH 7.8 surface of TTB is positively charged, whereas above pH 7.8 it is negatively charged. So, the adsorption of negatively charged anions like Cr(VI) and F^- is more at lower pH and less at higher pH. At pH more than 6, OH^- ions of the solution may compete with negatively charged adsorbate species and reduce the percentage of Cr(VI) or F^- adsorption. The effect of pH on % of Cr(VI) and F^- adsorption is shown in Fig. 3. pH of the solution was measured after each adsorption and is represented as final pH. The final pH increases with the increase in initial pH. The variation of final pH with respect to initial pH has been marked as dotted lines in Fig. 3.

The amount of adsorbate concentration either Cr(VI) or F^- in the solution was varied from 5 to 25 mg/L keeping all other parameters constant. As observed by other researchers [25], in this case also % of adsorption decreases from 87.23 to 27.49% for Cr(VI) and from 95.25 to 56.62% for F^- with the increase in adsorbate concentration. The result is shown in Fig. 4. Similarly, uptake increases from 0.8 to 1.4 mg/g for Cr(VI) and from 0.74 to 3.11 mg/g for F^- with the increase in either Cr(VI) or F^- ion concentration. The increase in adsorption with the increase in adsorbate ion concentration may be due to the higher probability of collision between the adsorbate and adsorbent surfaces. Here also, final pH of the solution increases with respect to Cr(VI) or F^- concentration shown as dotted lines in Fig. 4.

TTB concentration was varied from 5 to 30 g/L in experiments keeping all other parameters constant. In this case also, like most of the cases % of Cr(VI) and F^- adsorptions increase from 46.8 to 97.55% for Cr(VI) and from 59.15 to 97.7% for F^-. Similarly, Cr(VI) uptake decreases from 2.3 to 0.25 mg/g and F^- uptake from 2.9 to 0.24 mg/g with this variation. The same trend has been observed for the change in the final pH as before, and the final pH of the solution after adsorption with respect to TTB concentration is shown as dotted lines in Fig. 5.

Temperature of the system was varied from 30 to 60 °C keeping all other parameters constant. In both the cases, % of adsorption was decreased with the increase in temperature

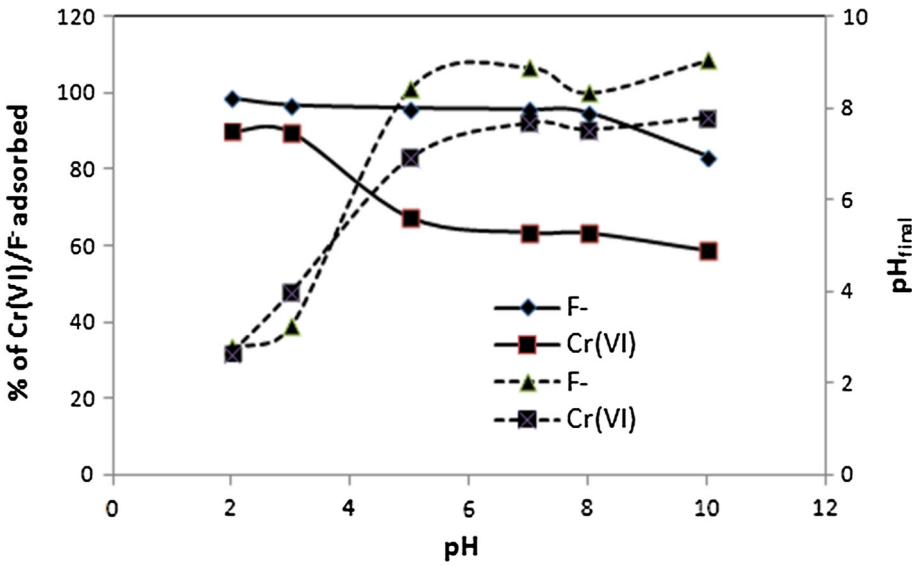

Fig. 3 Effect of pH on % of Cr(VI)/F^- adsorption (*solid lines*) variation of final pH with respect to initial pH of the solution (*dotted lines*)

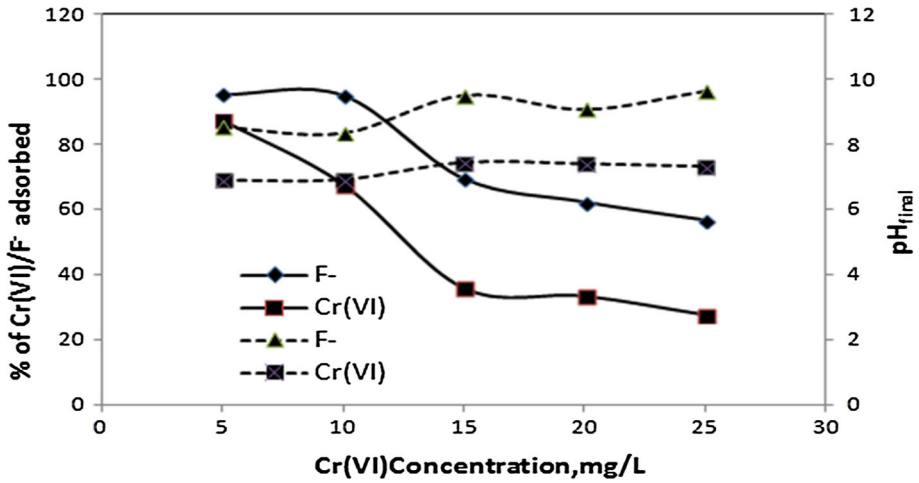

Fig. 4 Effect of $Cr(VI)/F^-$ concentration on % of adsorption (*solid lines*) variation of final pH with respect to $Cr(VI)/F^-$ concentrations (*dotted lines*)

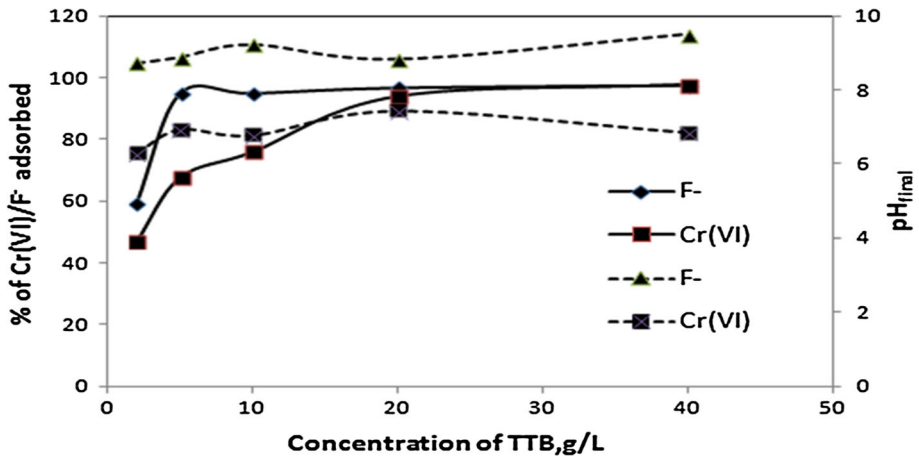

Fig. 5 Effect of TTB concentration on % of $Cr(VI)/F^-$ adsorption (*solid lines*) variation of final pH with respect to TTB concentrations (*dotted lines*)

as shown in Fig. 6. This may be due to the decomposition of adsorbent surface at higher temperatures. It may also be due to the exothermic nature of adsorption. Here also, pH of the solution after adsorption increases (final pH) with the increase in temperature shown as dotted lines in Fig. 6.

From temperature experiments, activation energies were determined using Arrhenius plot [27]. Other thermodynamic parameters such as entropy changes (ΔS), enthalpy changes (ΔH) and free energy changes (ΔG) were calculated by using the well-known thermodynamic relationship discussed earlier [28]. ΔH and ΔS were calculated by using the equation

$$\ln K_D = (\Delta S/R) - (\Delta H/RT) \tag{10}$$

where K_D distribution coefficient $= \frac{\text{Concentration of adsorbate on adsorbent (mg/g) at equilibrium}}{\text{Concentration of adsorbate in solution (mg/L) at equilibrium}}$, T temperature (K), R universal gas constant.

ΔH and ΔS were determined from the slopes and intercepts, respectively, of the plots drawn between $\ln K_D$ versus $1/T$. Again ΔG can be calculated by using the equation

$$\Delta G = \Delta H - T\Delta S \tag{11}$$

The activation energies and other thermodynamic parameters are shown in Table 1. The negative activation energies indicate ease and exothermic nature of the adsorption processes. Similarly, the negative values of enthalpy changes and free energy changes suggest that the Cr(VI) and F^- adsorptions on TTB are exothermic and spontaneous in nature, respectively. Exothermic adsorptions are physical in nature [29].

3.4 Adsorption Isotherms

Freundlich and Langmuir isotherm models [30,31] were applied to Cr(VI) and F^- adsorption on TTB surface. These two isotherms were determined by varying Cr(VI) or F^- concentration of the solutions from 5 to 25 mg/L at an adsorbent dose of 5 g/L.

The Freundlich isotherm equation is

$$\log q_e = \log K + (1/n) \log C_e \tag{12}$$

where q_e amount of $Cr(VI)/F^-$ adsorbed (mg/g) at equilibrium, C_e equilibrium concentration of $Cr(VI)/F^-$ in solution (mg/L), K constant related to adsorption capacity, n constant related to adsorption intensity.

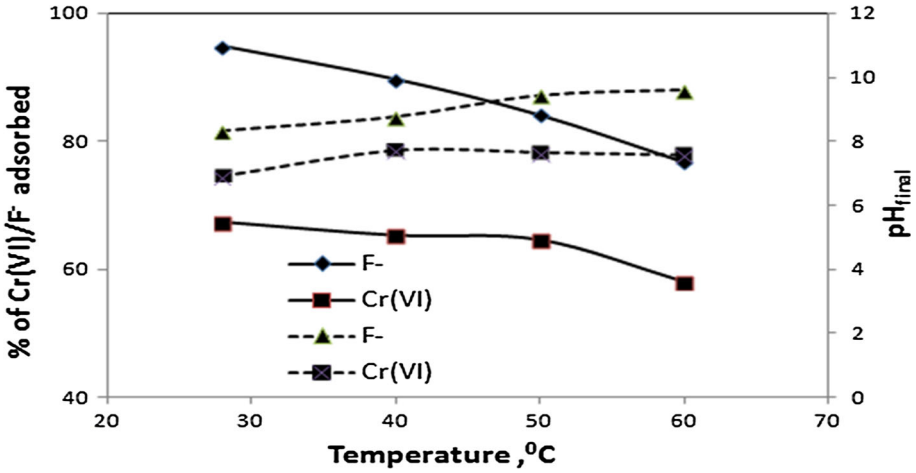

Fig. 6 Effect of temperature on % of Cr(VI)/F^- adsorption (*solid lines*) variation of final pH with respect to temperatures (*dotted lines*)

Table 1 Thermodynamic parameters

Temperature (K)	Activation energy (kJ/mol)		ΔH (kJ/mol)		ΔS (kJ/K mol)		ΔG (kJ/mol)	
	Cr(VI)	F^-	Cr(VI)	F^-	Cr(VI)	F^-	Cr(VI)	F^-
301	−73.73	−52.28	−9.49	−45.05	−0. 025	−0.125	−1.965	−7.43
313							−1.665	−5.93
323							−1.415	−4.68
333							−1.165	−3.43

When log q_e is plotted against log C_e, a straight line is obtained. K and n are determined from the intercepts and slopes of those straight lines, respectively.

The Langmuir adsorption isotherm is as follows

The equation is

$$C_e/q_e = 1/q_m b + C_e/q_m \tag{13}$$

where b constant related to energy of adsorption (L/mg), q_m adsorption capacity (mg/g).

b and q_m values were obtained from the intercepts and slopes, respectively, of the plots drawn between C_e/q_e and C_e. It has been observed that the correlation coefficient (R^2) values of Langmuir plots are higher than those of Freundlich plots. So, Langmuir isotherm is obeyed well compared to Freundlich isotherm in both the cases. The R^2 values of both the isotherms are shown in Table 2. The Langmuir adsorption capacity for F^- is higher in comparison with Cr(VI) as shown in Table 2. So, F^- adsorption on TTB is better in comparison with Cr(VI).

3.5 Adsorption Kinetics

The mechanism and the rate of adsorption are greatly dependent on physicochemical properties of the adsorbent. In adsorption studies, several kinetic models are proposed to examine the controlling mechanism of adsorption process. Data of both the adsorption processes were fitted to Lagergren's equation, Ho and Mc-Kay equation, Morris–Weber, Dubinin–Radushkevich (D.R.) and Temkin isotherms as follows [32]. Summary of different models is represented in Table 2.

3.5.1 Lagergren's or Pseudo-First-Order Equation

The equation is

$$\log(q_e - q_t) = \log(q_e) - (k_1/2.303)t \tag{14}$$

where q_t amount of Cr(VI)/F^- adsorbed per unit weight of adsorbent (mg/g) at time t, q_e amount of Cr(VI)/F^- ions adsorbed per unit weight of adsorbent (mg/g) at equilibrium, k_1 pseudo-first-order rate constant of adsorption.

A straight line would be obtained if a graph is plotted between log $(q_e - q_t)$ versus t. The rate constant (k_1) for pseudo-first-order reaction can be obtained from the slope of this graph.

3.5.2 Ho and Mc-Kay's or Pseudo-Second-Order Equation

The equation is

$$t/q_t = 1/(k_2 q_e^2) + (1/q_e)t \tag{15}$$

where k_2 is the equilibrium rate constant of pseudo-second-order equation.

A straight line would be obtained if a graph is plotted between t/q_t versus t. From the intercept of the plot, k_2 can be

Table 2 Summary of different isotherms studied

Kinetic/isotherm models studied	R^2		Inferences	
	Cr(VI)	F^-	Cr(VI)	F^-
Freundlich isotherm	0.13	0.67	–	–
Langmuir isotherm	0.95	0.93	Adsorption capacity = 1.38 mg/g	Adsorption capacity = 3.01 mg/g
			Langmuir isotherm constant, a constant related to energy of adsorption = 0.87 L/mg	Langmuir isotherm constant =1.02 L/mg
Lagergren's (pseudo-first-order) equation	0.7–0.9	0.00008–0.84	–	–
Ho and Mc-Kay (pseudo-second-order) equation	0.9–1	0.5–0.9	Rate constant varies from 0.04–8.04 1/M s	Rate constant varies from 0.07–7.78 1/M s
Morris–Weber equation	0.79–0.99	0.76–0.98	Intra-particle transport rate constant (R_{id}) = 0.005 to 0.124 mg/g/min$^{0.5}$	R_{id} = 0.091 to 0.314 mg/g/min$^{0.5}$
			High R^2 value indicates diffusion through the intra-particle to be the rate-limiting step	Here also diffusion through the intra-article is the rate-limiting step
			High R^2 values conclude better adsorption rate and adsorption mechanism	High R^2 values conclude better adsorption rate and adsorption mechanism
The Dubinin–Radushkevich (D.R.) isotherm	0.76–0.99	0.903–0.908	Adsorption energies in between 0.26 and 2.8 J/mol, suggested physical nature of adsorption	Adsorption energies in between 0.31 and 0.35 J/mol, suggested physical nature of adsorption
Temkin isotherm model	0.98–0.99	0.89–0.90	Heat of sorption varies from 0.21 to 0.58 J/mol indicates physical nature of adsorption	Heat of sorption varies from 0.88 to 1.16 J/mol also indicates physical nature of adsorption

obtained. From the R^2 values of both pseudo-first-order and pseudo-second-order equations, it has been concluded that second order is a better fit for both Cr(VI) and F^- adsorption. Rate constants and R^2 values are shown in Table 2. It indicates the dependence of the adsorption rate on both adsorbent surface and adsorbate.

3.5.3 Weber Morris Equation

It explains well the intra-particle diffusion model of the adsorption reactions.

The equation is

$$q_t = R_{id}\, t^{1/2} \tag{16}$$

where q_t amount of Cr(VI)/F^- ions adsorbed per unit weight of adsorbent (mg/g), R_{id} intra-particle transport rate constant (mg/g/min$^{0.5}$), T time (min).

A straight line would be obtained if a graph is plotted between q_t versus $t^{1/2}$. The slope of the graph gives R_{id}, and the rate constant of intra-particle transport and the values are shown in Table 2. High R^2 values in both Cr(VI) and F^- adsorption cases indicate the better understanding of this isotherm and diffusion through the intra-particle is the rate-limiting step.

3.5.4 The Dubinin–Radushkevich (D.R.) Isotherm

In linear form, D.R. isotherm is

$$\ln q_e = \ln X'_m - K'\epsilon^2 \tag{17}$$

where ϵ Polanyi potential $= RT\ln(1 + 1/C_e)$, q_e amount of Cr(VI)/F^- ions adsorbed per unit weight of adsorbent (mg/g) at equilibrium, X'_m adsorption capacity of the adsorbent (mg/g), C_e equilibrium concentration of adsorbate ions in solution (mg/L), K' constant related to adsorption energy (mol^2/ kJ^2), R gas constant (kJ/K/mol), T temperature (K).

A plot between $\ln q_e$ versus ϵ^2 gives a straight line. The slope and intercept of the plot gives constants related to adsorption energy (K') and adsorption capacity (X'_m), respectively.

The mean adsorption energy $(E) = (2K')^{-1/2}$ (18)

Adsorption energy values of both the adsorptions are shown in Table 2. Adsorption energies of both the adsorption processes are found to be less than 8 kJ/mol. It indicates physical nature of adsorption [33].

3.5.5 Temkin Isotherm Model

How adsorbate interacts with the adsorbent in the adsorption process is explained by this isotherm and is given by

$$q_e = B \ln A_T + B \ln C_e \quad (19)$$

where q_e amount of Cr(VI)/F^- ions adsorbed per unit weight of adsorbent (mg/g) at equilibrium, B constant related to heat of sorption (J/mol), A_T Temkin isotherm equilibrium binding constant (L/g), C_e concentration ofmetal ions in solution (mg/L) at equilibrium.

The above equation is equivalent to equation of straight line. The slope of the straight line plotted between q_e and $\ln C_e$ gives B, a constant related to heat of sorption. The heat of sorption values are shown in Table 2 and shows physical nature of both the adsorptions [34].

3.6 Effect of Co-ions

Effect of presence of other co-ions (cations and anions) on Cr(VI) or F^- ion adsorption on TTB was studied by adding different electrolytes such as $NaNO_3$, $Mg(NO_3)_2 \cdot 6H_2O$, $Al(NO_3)_3 \cdot 9H_2O$, NaCl, Na_2SO_4 and $Na_2HPO_4 \cdot 2H_2O$ in varying concentrations (0.01–0.15 M) separately to the solution containing 10 mg/L of either Cr(VI) or F^- . These electrolytes provide cations such as Na^+, Mg^{2+}, Al^{3+} and anions such as Cl^-, NO_3^-, SO_4^{2-} and PO_4^{3-}(formation of HPO_4^{2-} is ignored). These are the ions which are commonly present along with different toxic elements in different industrial wastewaters.

In order to compare the effect of different co-cations, $NaNO_3$, $Mg(NO_3)_2$ and $Al(NO_3)_3$ were taken into consideration. These electrolytes provide cations Na^+, Mg^{2+} and Al^{3+} where cationic charges are +1, +2 and + 3, respectively, with the same anion nitrate. It has been observed from Figs. 7 and 8 that interference increases in the order $Al(NO_3)_3 < Mg(NO_3)_2 < NaNO_3$. It is clearly understood from the result that interference is directly proportional to the size of the cations or solubility of the electrolytes and inversely proportional to the charge on the cations and bond dissociation energy of the electrolytes. The same trend has been observed for both Cr(VI) and F^- adsorption.

In order to study the effect of other co-anions on Cr(VI) or F^- adsorption, three different electrolytes such as NaCl, Na_2SO_4, Na_2HPO_4 having same cation with different anions were taken. These are the electrolytes which provide anions like Cl^-, SO_4^{2-} and PO_4^{3-} having -1, -2 and -3 charges, respectively. It has been observed from the graphs (Figures 9 and 10) that Cr(VI) or F^- adsorption is greatly interfered in the presence of anions due to competition. Higher the charge on the anions higher is the interference. The interference of these three electrolytes follow the order $Na_2HPO_4 > Na_2SO_4 > NaCl$ and the % of both Cr(VI) and F^- adsorption follow the reverse order.

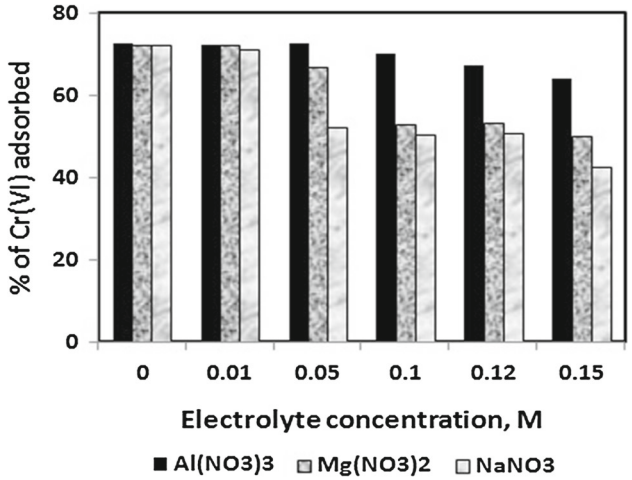

Fig. 7 Effect of $NaNO_3$, $Mg(NO_3)_2$ and $Al(NO_3)_3$ on Cr(VI) adsorption

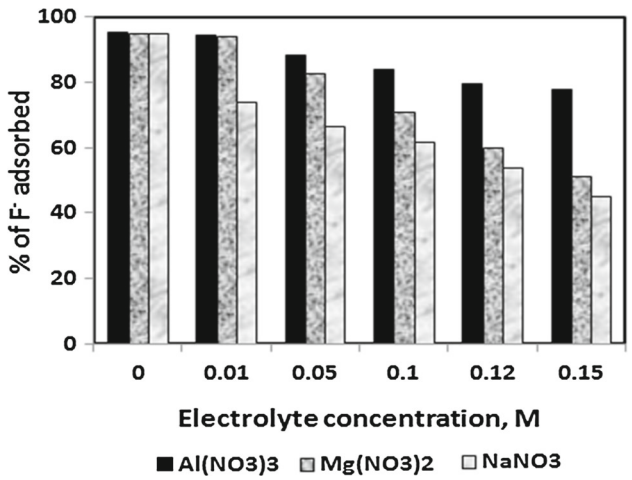

Fig. 8 Effect of $NaNO_3$, $Mg(NO_3)_2$ and $Al(NO_3)_3$ on F^- adsorption

4 Conclusions

Bauxite treated at 400 °C (TTB) is found to be an effective remover of both Cr(VI) and F^- from aqueous solution. The optimum conditions for adsorption are stirring speed—200 rpm, temperature—30 °C, contact time—120 min for

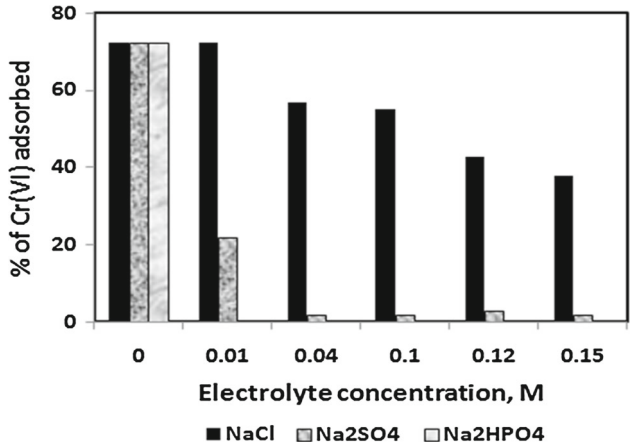

Fig. 9 Effect of NaCl, Na_2SO_4 and Na_2HPO_4 on Cr(VI) adsorption

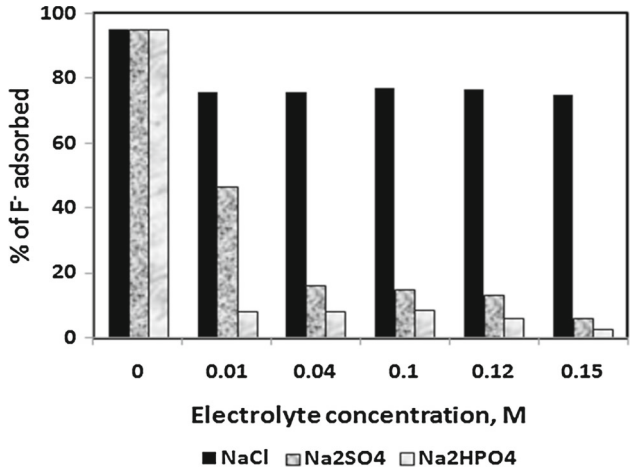

Fig. 10 Effect of NaCl, Na_2SO_4 and Na_2HPO_4 on F^- adsorption

Cr(VI) and 180 min for F^-. Cr(VI) adsorption is maximum within pH 2–3, whereas very little variation in adsorption is there within pH 2–8 for F^-. In both the adsorption cases, activation energies were found to be negative (−73.73 kJ/mol for Cr(VI) and −52.28 kJ/mol for F^-) which indicate exothermic nature of the processes. Interpretation to different kinetic models concludes the physicochemical nature of both the adsorptions. The nature of both the adsorption processes is similar in all respects. In a single step batch method, the uptake of Cr(VI) and F^- on TTB is found to be 1.38 and 3.01 mg/g, respectively, which can be further increased by performing the same study in a cyclic or column manner. TTB is a better adsorbent for F^- compared to Cr(VI). Both Cr(VI) and F^- adsorptions on TTB are affected by the presence of both cationic and anionic co-ions. The interference in the presence of co-ions is directly proportional to size of both the ions and charge on the anions and inversely proportional to the charge on the cations. This small-scale adsorption study can be extended to field scale using real industrial wastewaters.

Acknowledgements The authors are very much thankful to The President, Siksha 'O' Anusandhan University, Bhubaneswar, for his permission to publish this paper. One of the authors (MRG) thanks the Authorities of this University for providing her a research fellowship.

References

1. Ageena, N.A.: The use of local sawdust as an adsorbent for the removal of copper ion from wastewater using fixed bed adsorption. J. Eng. Technol. **28**(2), 224–235 (2010)
2. Chopra, A.K.; Pathak, C.; Prasad, G.: Scenario of heavy metal contamination in agricultural soil and its management. J. Appl. Nat. Sci. **1**(1), 99–108 (2009)
3. Brungesh, K.V.; Nagabhushana, B.M.; Raveendra, R.S.; HariKrishna, R.; Prashantha, P.A.; Nagabhushana, H.: Adsorption of Cr(VI) from aqueous solution onto a mesoporous carbonaceous material prepared from naturally occurring *Pongamia pinnata* seeds. J. Environ. Anal. Toxicol. **5**(6), 1–7 (2015)
4. Igwe, J.C.; Abia, A.A.: Competitive adsorption of Zn(II), Cd(II) and Pb(II) ions from aqueous and non-aqueous solution by maize cob husk. Afr. J. Biotechnol. **4**(10), 1113–1114 (2005)
5. Kugali, N.M.; Yadawe, M.S.: Pollution of drinking water due to fluoride and dental fluorosis at Hunagundtaluk of Bagalkot district, Karnataka. Int. J. Appl. Biol. Pharm. **1**(2), 322–328 (2010)
6. Tewari, A.; Dubey, A.; Chaturvedi, M.K.: Assessment of exposure, intake and toxicity of fluoride from ground water source. Rasayan J. Chem. **5**(2), 199–202 (2012)
7. Arlappa, N.; Qureshi, A.; Srinivas, R.: Fluorosis in India: overview. Int. J. Res. Dev. Health **1**(2), 97–102 (2013)
8. Tlanquo, L.; Daolei, X.; Chanqhua, H.; Xiaojun, X.; Huanq, B.; Rui, N.; Shuli, L.; Zhenqyanq, D.; Wei, L.: Simultaneous adsorption of fluoride and hexavalent chromium by synthetic mesoporous alumina: performance and interaction mechanism. RSC Adv. **6**, 48610–48619 (2016)
9. Singh, R.; Gautam, N.; Mishra, A.; Gupta, R.: Heavy metals and living systems: an overview. Indian J. Pharmacol. **43**(3), 246–253 (2011)
10. Salunke, B.; Raut, S.J.: Removal of heavy metal Ni(II) and Cr(VI) from aqueous solution by scolecite natural zeolite. Int. J. Chem. Sci. **10**(2), 1133–1148 (2012)
11. Vidal, M.; Santos, M.J.; Abrao, T.; Rodriguez, J.; Rigol, A.: Modeling competitive metal sorption in a mineral soil. Geoderma **149**, 189–198 (2009)
12. Vistaso, E.; Theng, B.K.G.; Bolan, N.S.; Parfitt, R.L.; Mora, M.L.: Competitive sorption of molybdate and phosphate in andisols. J. Soil Sci. Plant Nutr. **12**, 59–72 (2012)
13. Bayaa, E.I.; AlKhalik, N.A.; Alkhalik, E.A.: Effect of ionic strength on the adsorption of copper and chromium ions by vermiculite pure clay mineral. J. Hazard Mater. **170**, 1204–1209 (2009)
14. Boudrahem, F.; Benissad, F.A.; Soualah, A.: Adsorption of lead(II) from aqueous solution by using leaves of date trees as an adsorbent. J. Chem. Eng. Data **56**, 1804–1812 (2011)
15. Yang, S.T.; Sheng, G.D.; Guo, Z.Q.; Tan, X.L.; Xu, J.Z.; Wang, X.K.: Investigation of radionuclide 63 Ni(II) sequestration mechanisms on mordenite by batch and EXAFS spectroscopy study. Sci. China Chem. **42**, 844–855 (2012)
16. Pathak, P.D.; Mandavgane, S.A.; Kulkarni, B.D.: Characterizing fruit and vegetable peels as bioadsorbents. Curr. Sci. **110**(11), 2114–2123 (2012)
17. Egbuna, S.O.; Ugadu, E.; Ujam, A.: Effects of thermal activation on the physico-chemical properties of natural white clay as a local adsorbent. Int. J. Eng. Sci. Invent. **3**(11), 37–48 (2014)
18. Onchoke, K.K.; Sasu, S.A.: Determination of hexavalent chromium Cr(VI) concentrations via ion chromatography and UV–Vis spec-

trophotometry in samples collected from Nacogdoches wastewater treatment, East Texas (USA). Adv. Environ. Chem. (2016). doi:10.1155/2016/3468635
19. Tembhurkar, A.R.; Dongre, S.: Studies on fluoride removal using adsorption process. J. Environ. Sci. Eng. **48**(3), 151–156 (2006)
20. Erdem, M.; Altundogan, H.S.; Tumen, F.: Removal of hexavalent chromium by using heat-activated bauxite. Miner. Eng. **17**, 1045–1052 (2004)
21. Urai, J.L.; Feenstra, A.: Weakening associated with the diaspore–corundum dehydration reaction in metabauxites: an example from Naxos (Greece). J. Struct. Geol. **23**, 941–950 (2001)
22. Som, S.K.; Bhattacharya, A.K.: Mineralogy of Panchpatmali bauxite deposit based on XRD, IR, DTA and SEM studies. J. Geol. Soc. India **45**, 427–432 (1995)
23. Chromate and dichromate, Wikipedia, the free encyclopedia.
24. Prakash, S.; Das, B.: Surface properties of Indian hematite and bauxite and their coating mechanism with colloidal magnetite. J. Sci. Ind. Res. **58**, 436–442 (1999)
25. Thilagavathy, P.; Santhi, T.: Adsorption of Cr(VI) onto low-cost adsorbent developed from Acacia nilotica leaf activated with phosphoric acid: kinetic, equilibrium isotherm and thermodynamic studies. Int. J. Sci. Res. **3**, 308–314 (2014)
26. Samdani, S.; Attar, S.J.; Kadam, C.; Baral, S.S.: Treatment of Cr(VI) contaminated waste water using biosorbent, *Hydrilla verticillata*. Ind. J. Eng. Res. Ind. Appl. **1**(4), 271–282 (2008)
27. Gude, S.M.; Das, S.N.: Adsorption of Cr(VI) from aqueous solutions by chemically treated water hyacinth *Eichhornia crassipes*. Int. J. Chem. Technol. **15**, 12–18 (2008)
28. Gandhi, N.; Sirisha, D.; Chandra Sekhar, K.B.: Adsorption of Cr(VI) from aqueous solution by using multani miti. Int. J. Res. Pharm. Chem. **4**(1), 168–180 (2008)
29. Ghosh, M.R.; Mishra, S.P.: Adsorption of Cr(VI) by using HCl modified *Lagenaria siceraria* peel (HLSP). J. Mater. Environ. Sci. **7**(8), 3050–3060 (2016)
30. Ratnamala, G.M.; Deshannava, U.B.; Munyal, S.; Tashildar, K.; Patil, S.; Shinde, A.: Adsorption of reactive blue dye from aqueous solutions using sawdust as adsorbent: optimization, kinetic, and equilibrium studies. Arab. J. Sci. Eng. **41**, 333–344 (2016)
31. Arivoli, S.; Nandhakumar, V.; Saravanan, S.; Nagarajan, S.: Adsorption dynamics of copper ion by low cost activated carbon. Arab. J. Sci. Eng. **34**, 1–12 (2009)
32. Wang, X.S.; Li, Z.Z.; Tao, S.R.: Removal of Cr(VI) from aqueous solution using walnut hull. J. Environ. Manag. **90**, 721–729 (2009)
33. Das, B.; Mondal, N.; Roy, P.; Chattaraj, S.: Equilibrium kinetics and thermodynamic study on Cr(VI) removal from aqueous solution using *Pistia stratiotes* biomass. Chem. Sci. Trans. **2**, 85–104 (2013)
34. Pragathiswaran, C.; Sibi, S.; Sivanesan, P.: Comparison studies of various adsorption isotherms for aloe vera adsorbent. Int. J. Res. Pharm. Chem. **3**, 886–889 (2013)